arXiv:1609.06541v1 [cond-mat.soft] 21 Sep 2016

Mean-field beyond mean-field: the single particle view for moderately to strongly coupled charged fluids

Ladislav Šamaj
Institute of Physics, Slovak Academy of Sciences, Bratislava, Slovakia

Alexandre P. dos Santos and Yan Levin
Instituto de Física, Universidade Federal do Rio Grande do Sul, CP 15051, CEP 91501-970 Porto Alegre, RS, Brazil

Emmanuel Trizac
LPTMS, CNRS, Univ. Paris-Sud, Université Paris-Saclay, 91405 Orsay, France

(Dated: September 22, 2016)

In a counter-ion only charged fluid, Coulomb coupling is quantified by a single dimensionless parameter. Yet, the theoretical treatment of moderately to strongly coupled charged fluids is a difficult task, central to the understanding of a wealth of soft matter problems, including biological systems. We show that the corresponding coupling regime can be remarkably well described by a single particle treatment, which, at variance with previous works, takes due account of inter-ionic interactions. To this end, the prototypical problem of a planar charged dielectric interface is worked out. Testing our predictions against Monte Carlo simulation data reveals an excellent agreement.

PACS numbers: 82.70.-y, 82.45.-h, 61.20.Qg

I. INTRODUCTION

Charged fluids are abundant in man-made or natural systems, in which thermalized mobile ions interact via Coulomb forces collectively, and also with more macroscopic charged bodies such as colloids, proteins, or DNA. The first theoretical attempt for describing inhomogeneous Coulomb fluids dates back about a century ago, to pioneering works of Gouy in Lyon [1] and Chapman in Oxford [2]. These predate the Debye and Hückel approach which aimed at accounting for the unusual thermodynamic properties of electrolytes like NaCl, where dissociation leads to a fluid of Na^+ and Cl^- ions in water [3]. These early treatments are all mean-field in spirit. It was realized in the 1980s that by discarding electrostatic correlations, mean-field theory precludes some counter-intuitive effects such as the electrostatic attraction of like charge surfaces, revealed by experiments, simulations, and theoretical approaches, see [4–12] and references therein. It is now recognized that the validity of mean-field treatments, epitomized by the Poisson-Boltzmann theory of extensive use in colloid science [14], requires the necessary condition of sufficiently small electrostatic coupling; in the language of the coupling parameter Ξ to be defined below and which pits electrostatic against thermal energies, this means $\Xi \ll 1$ up to $\Xi \simeq 1$. On the other hand, systems with moderate to strong coupling are profuse, starting with nucleic acids and cell membranes in aqueous solutions. Charges are pivotal to their stability *in vivo*. The study of these biological objects from a physics perspective has rekindled interest in Coulomb fluids, with particular emphasis on strong coupling regime. Yet, analytical progress for moderately to strongly coupled charged fluids has proven elusive, as will be illustrated below. Our goal here is to fill this gap, with a theoretical treatment that is both physically transparent, and remarkably accurate. It takes advantage of the existence of a correlation hole around individual ions in the system, a well known feature, that has nevertheless not been turned into an explicit analytical treatment so far. It is also relevant to emphasize from the outset that our approach deals with salt-free systems, where only counterions are present in the solution. This situation, with no added buffer electrolyte, applies to deionized suspensions (see e.g. the experiments reported in [15]).

II. LENGTH SCALE SEPARATION

The limit of asymptotically large couplings admits a simple description, in elementary settings such as that sketched in Fig. 1-a. It can be understood by a length scale analysis, which we now illustrate on the emblematic primitive counter-ion only model. For strongly charged plates, most counterions remain in a close vicinity of the surface. The characteristic distance a between the condensed counter-ions is ruled by electro-neutrality: $\sigma a^2 \propto q$, where σe is the plate surface charge density at $z = 0$ and $-qe$ is the ion's charge, with e the elementary charge. The typical extension, or excursion of the counter-ions from the surface, is denoted μ. This quantity, named the Gouy length, follows by the balance of thermal energy kT with the energy of an ion $-qe$ at position z, $\mu = \varepsilon\, kT/(2\pi q\sigma e^2)$. The dimensionless

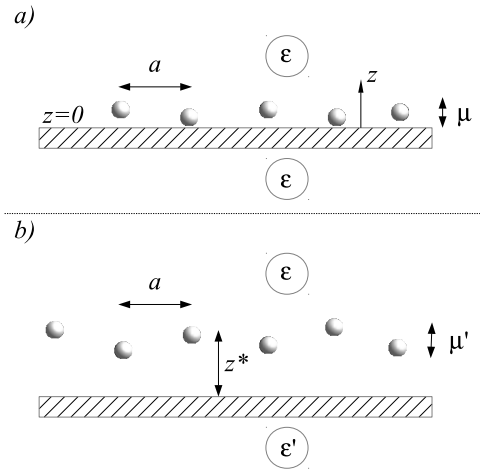

FIG. 1. Schematic side view of the system, without (panel a) and with (panel b) dielectric mismatch. The mobile counter-ions, point-like, are drawn as spheres for the sake of illustration. In a), the dielectric constant of the solvent (ε) and that of the interface (ε') are equal. We will also consider in b) the case where both constants differ, for which the dielectric mismatch is quantified by $\Delta = (\varepsilon - \varepsilon')/(\varepsilon + \varepsilon')$. Panels a) and b) depict regimes of large Coulomb coupling ($\Xi \gg 1$). Then, the characteristic distance a between the counter-ions is set by electro-neutrality: $\sigma a^2 \propto q$, where σe is the plate surface charge density at $z = 0$ and $-qe$ is the ion's charge, with e the elementary charge. The typical extension μ follows by balancing thermal energy kT with the energy of an ion $-qe$ at position z in the potential $-2\pi\sigma e z/\varepsilon$ created by the bare plate: $\mu = \varepsilon\, kT/(2\pi q\sigma e^2)$, the so-called Gouy length. The coupling parameter is defined as $\Xi = 2\pi\sigma q^3 e^4/(\epsilon kT)^2$. Thus, $\Xi \propto a^2/\mu^2$ and $\Xi \gg 1 \Rightarrow \mu \ll a$. In panel b), repulsive dielectric images should be considered ($\varepsilon' < \varepsilon$) and a depletion zone of size z^* appears. The typical extension of the profile, μ', is no longer given by μ [16].

coupling parameter, defined as $\Xi = 2\pi\sigma q^3 e^4/(\epsilon kT)^2$, is proportional to a^2/μ^2. When $\Xi \gg 1$, Coulomb interaction between the counter-ion exceeds thermal energy, so that the mobile counter-ions in the vicinity of a plate are strongly attracted to the surface, and at the same time repelled from the adjacent counterions, $\Xi \gg 1 \Rightarrow \mu \ll a$. This results in a correlation hole size a [17, 18], exceeding a typical transverse excursion of a counter-ios from the surface characterized by the Gouy length μ, see Figure 1-a, where the key length scales are depicted. For colloidal particles with bare charge $Z = 10^4 e$ and radius of $R = 10^3$ Å, in aqueous solution, the coupling parameter is $\Xi \approx 0.26$ for monovalent counterions ($q = 1$), 2.1 for divalent counter-ions, and 7.0 for trivalent counter-ions. However, since Ξ is inversely proportional to the square of the dielectric constant, for solvents of lower dielectric constants such as mixtures containing water and alcohol, Ξ can easily reach 50 for moderately charged surfaces with trivalent counterions. It is also relevant to provide reasonable bounds for the possible values of Ξ, as a function of valence q. In water at room temperature, highly charged interfaces have σe on the order of one e per namometer square, and therefore Ξ is on the order of q^3. With trivalent ions, this means $\Xi \simeq 30$, which is already way into the regime covered by our treatment.

The length scale separation provides the grounds for a surprisingly simple picture of a strongly correlated Coulomb system where the ions react mostly to the bare plate potential, while ion-ion interactions become insignificant as $\Xi \to \infty$ [11, 12, 18]. Thus, the ionic density profile takes an exponential form $\rho(z) \propto \exp(-z/\mu)$ characteristic of a particle in a constant field. The proportionality factor can be determined by the contact value theorem [13]. This "ideal gas" barometric law has been fully validated by numerical simulations [19, 20]. Corrections beyond the ideal gas regime can be computed in a $1/\sqrt{\Xi}$ expansion by a perturbation around the Wigner crystal [21], that forms when Ξ exceeds some (very large) crystallization value $\Xi_c \simeq 3.10^4$ [22].

It is generally believed that single particle ideas fail in situations where scale separation no longer holds: for instance if Ξ is in some crossover regime of moderate coupling or in the situation of Fig. 1-b) with a dielectric mismatch. We shall see that although the ideal gas view indeed severely breaks down in these generic cases – which as a matter of fact significantly limits its practical interest – a "correlation hole modified" single-particle treatment can be effectively applied. It is our purpose to present this fully analytical, self-consistent approach. The theory developed here allows to accurately determine the counter-ion density distribution ρ, which is in striking agreement with computer simulation results. This leads to an unexpected conclusion that somewhat beyond the usual mean-field regime of weakly coupled fluids, an even simpler mean-field provides a quantitative description. In the limiting cases where the ideal gas formulation is relevant, our analysis recovers it.

III. CORRELATION HOLE: TREATMENT AND CONSEQUENCES

We now address the simplest geometry where lack of scale separation forestalls the ideal gas single particle physics: the planar interface alluded to above, with a dielectric jump between the solvent (dielectric constant ε) and the confining charged body (dielectric constant ϵ') occupying the lower half space as shown in Figure 1-b. Although simplified, such a geometry provides a paradigmatic testbed to shape intuition and theoretical ideas. The situation $\Delta = (\varepsilon - \varepsilon')/(\varepsilon + \varepsilon') > 0$ is the most relevant one, since the dielectric constant of materials like glass, proteins, or polarizable colloids is much smaller than that of water: each charge admits an image of the same sign [23], with a resulting repulsive interaction. It also encompasses the air-liquid interfaces, for which $\varepsilon/\varepsilon' \simeq 80$. The case $\Delta < 0$ leads to attractive images [24], and to the disappearance of the depletion zone in Fig. 1-b. The extreme limit corresponds to a grounded electrode with $\varepsilon' \to \infty$ for which $\Delta = -1$. In this case the ions can no longer be modeled as point particles and a hardcore must be introduced. In this paper we will restrict our attention to systems with $\Delta > 0$.

The mobile ions are attracted to the oppositely charged interface at $z = 0$, but concomitantly each charge $-qe$ at position z has a dielectric image of charge $-qe\Delta$ at $-z$ [23], which strongly repels it. A depletion zone ensues [25]; it is quite straightforward to estimate its size z^*, which turns out to be of the same order as a. Thus, one can no longer consider that ions are far from each other compared to their distance to the plate: the intrusion of a new length scale, z^*, explains the failure of the single particle ideal gas picture. Nevertheless, the ionic profile's extension, μ', remains the smallest length scale of the problem [16]. Hence, we are led to neglect the correlations between the ion's fluctuations, while taking due account of their interactions in an effective way, at variance with the ideal gas formulation. The problem we face reduces to computing the effective potential u that a given ion experiences, when at a distance z away from the interface. When known, u directly leads, through a Boltzmann weight, to the main quantity of interest, the density profile: $\rho(z) \propto \exp(-\beta u)$, $\beta = 1/(kT)$ being the inverse temperature. We emphasize that when explicit analitic expressions are sought, the state of the art lies in the single particle ideal gas view, in which case the potential of mean-force u stems from the force due to the plate at $z = 0$ and the test particle image charge [11, 12, 19, 26]. We shall see that this treatment is inappropriate for $\Delta \neq 0$, so that there is no analytical treatment available in the literature to study this general case. We attempt here to fill the gap. In other words, while the idea of correlation holes in more or less correlated Coulombic fluids is not novel [8, 10, 17, 18, 27–30], transforming the corresponding insight into a fully analytical theory is new; it is the subject of our paper.

Since practically relevant values of the coupling parameter are orders of magnitude smaller than the crystallization threshold, we envision the ions as forming a liquid, essentially two dimensional since we do not aim at covering the limit of too small Ξ (we will address the range $\Xi > 10$ here [31]). The key structural features of this liquid are embodied in the pair correlation function $g(r)$ [32, 33], a function of inter-ion distance providing the density of neighbors. This $g(r)$ is more or less structured depending on the value of Ξ [19], but is always strongly depleted at small distances r due to the strong Coulomb repulsion [17, 27, 30, 34–36]: we recover the correlation hole depicted in Fig. 1. A second characteristics is that the size of this hole is essentially Ξ-independent: being set by electro-neutrality, it is always given by the length scale a introduced in the caption of Fig. 1 [19]; besides, each particle has a coordination six [37]. We claim that these gross features are sufficient for a proper account of the ionic profile, without inclusion of further details. Two levels of simplification will be provided, having in common the existence of a correlation hole around the test particle, in the form of a concentric disk. 1) Apart from the test particle, the fluid of counter-ions is assumed structureless beyond R_0 (meaning $g(r) = 1$ for $r > R_0$). The size of the hole is set by balancing the hole and ion charges: $\pi R_0^2 \sigma e = qe$. This leads to a system of a moving ion in the field of a plate at $z = 0$, a punctured plate at z^* having a circular hole of size R_0, plus the dielectric images of all charges, of the same sign but weighted with a prefactor Δ, and located at the symmetric position with respect to the mid plane at $z = 0$. We call this route the correlation hole + strong coupling with zero neighbor (ch_0). 2) In a refined approach, we set $g(r) = 1$ beyond the first neighbors. Then, each particle with its 6 neighbors is in the center of a hole with radius R_6, now such that $\pi\sigma R_6^2 = q + 6q = 7q$. Due account of image charges leads to the model represented in Figure 2, referred to as ch_6. For both ch_0 and ch_6 routes, the process of smearing out an infinite number of counter-ions leads to a punctured charged plate, with a hole concentric with the test ion. Its interaction with the test particle is essential for a good account of the density profile.

IV. RESULTS

To explore the range of validity of the theory all the results will be compared with the Monte Carlo simulations performed using the 3D Ewald summation with a correction for slab geometry and for surface polarization. More details regarding simulations can be found in Refs. [44] and [45]. An interested reader can also consult an efficient implementation of slab geometry simulations for charged interfaces which has recently been developed in Ref. [46].

The analysis now proceeds in two steps [38]. First, the optimal distance z^* is derived, which yields the maximum

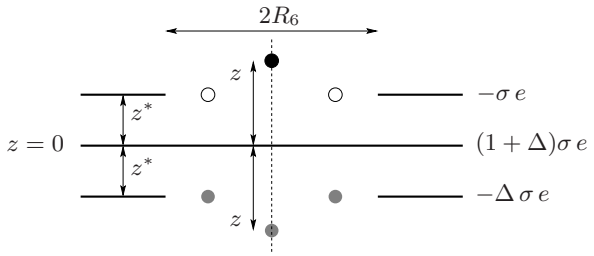

FIG. 2. Schematics of the ch_6 approach. A test particle (filled disc) is singled out at elevation z. Other counter-ions are assumed to be at their typical location z^*. Upon smearing out the counter-ions beyond a cutoff distance R_6, one obtains a *punctured* plate with charge density $-\sigma e$. The empty circles stand for the 6 nearest neighbors of the test particle. The symmetrically located dielectric images – discrete (displayed in gray) or continuous – are also shown. The simplified ch_0 view leads to a very similar setup, with the difference that there are no discrete neighbors: these ions are also smeared out, so that the hole becomes smaller, of radius $R_0 = R_6/\sqrt{7}$.

of the ionic profile $\rho(z)$. Second, the effective one-particle potential u is computed. For the sake of simplicity, we start by presenting the ch_0 approach. We fix all ions at $z = z^*$ (including the test particle), and calculate E_0, the energy per particle of the system, made up of 3 charged planes, two of which are punctured and located at $\pm z^*$, and 2 discrete charges (image included). It proves convenient to add and subtract to the image plane at $z = -z^*$, the potential of a charged disc with same density as the plate, $-\Delta\sigma e$. In doing so, one obtains a non-punctuated plate at $z = -z^*$, and a disc of charge density $\Delta\sigma e$, with radius R_0. The resulting energy per particle is

$$\begin{aligned} E_0(z^*) &= \frac{2\pi}{\varepsilon}\,(1+\Delta)\,\sigma q\, e^2 z^* \,-\frac{1}{2}\,\Delta\,\frac{2\pi}{\varepsilon}\,\sigma q\, e^2(2z^*) \,-\,\frac{1}{2}\Delta q\sigma\frac{e^2}{\varepsilon}\int_0^{R_0} dr\,\frac{2\pi r}{\sqrt{r^2+(2z^*)^2}} + \frac{q^2e^2}{2\varepsilon}\Delta\frac{1}{2z^*} \\ &= \frac{2\pi}{\varepsilon}\,\sigma q\, e^2 z^* + \frac{q^2e^2}{2\varepsilon}\Delta\frac{1}{2z^*} \,-\,\pi\Delta\, q\,\sigma\frac{e^2}{\varepsilon}\left[\sqrt{R_0^2+(2z^*)^2}-2z^*\right]. \end{aligned} \tag{1}$$

Turning to the ch_6 case, we have to consider 3 charged planes, two of which are punctured and located at $\pm z^*$, and 14 discrete charges. Proceeding along similar lines as above, the energy per particle now reads:

$$\begin{aligned} E_0(z^*) =& \frac{2\pi}{\varepsilon}\,\sigma q\, e^2 z^* + \frac{q^2e^2}{2\varepsilon}\Delta\left[\frac{1}{2z^*}+\frac{6}{\sqrt{a^2+4z^{*2}}}\right] \\ & -\pi\Delta\, q\,\sigma\frac{e^2}{\varepsilon}\left[\sqrt{R_6^2+(2z^*)^2}-2z^*\right]. \end{aligned} \tag{2}$$

Introducing the dimensionless variable $t = 2z^*/a$ where $a = 3^{-1/4}\sqrt{2q/\sigma}$ [39] and minimizing E_0 with respect to t, we have to solve

$$1-\Delta\left[\frac{t}{\sqrt{(R_6/a)^2+t^2}}-1\right] = \frac{\sqrt{3}}{4\pi}\left[\frac{\Delta}{t^2}\,+\,\frac{6\,\Delta\, t}{(1+t^2)^{3/2}}\right].$$

Once t and thus the depletion zone extension z^* is found, we have to dissociate the test particle from the ionic layer, move it along the z axis as depicted in Fig. 2, and compute the resulting potential $u(z)$. This is another elementary electrostatics exercise [40], with the result:

$$\begin{aligned} \beta u(z) \;=\; & (1+\Delta)\,\widetilde{z} \,+\, \frac{\Xi\Delta}{4\,\widetilde{z}} \\ & -\sqrt{\left(\widetilde{R}_6\right)^2+(\widetilde{z}-\widetilde{z}^*)^2} \,-\, \Delta\sqrt{\left(\widetilde{R}_6\right)^2+(\widetilde{z}+\widetilde{z}^*)^2} \\ & +\frac{6\,\Xi}{\sqrt{\widetilde{a}^{\,2}+(\widetilde{z}-\widetilde{z}^*)^2}} \,+\, \frac{6\,\Xi\,\Delta}{\sqrt{\widetilde{a}^{\,2}+(\widetilde{z}+\widetilde{z}^*)^2}} \end{aligned} \tag{3}$$

where tilde distances are rescaled by the Gouy length, e.g. $\tilde{z} = z/\mu$. The ch_0 counterpart of Eq. (3) is again very similar, without the last two terms in $6\,\Xi$ and with the substitution $\widetilde{R}_6 \to \widetilde{R}_0$ for the hole size. Since $\widetilde{R}_6^2 = 14\,\Xi$, we

have $\widetilde{R}_0^2 = 2\,\Xi$. Finally, the suitably normalized Boltzmann weight is the density profile sought for:

$$\rho(z) \;=\; \frac{\sigma}{q}\,\frac{e^{-\beta u(z)}}{\int e^{-\beta u(z')}dz'}. \tag{4}$$

By accounting solely for the interaction with the plate at $z = 0$ and with the test particle image, one has $\beta u = (1+\Delta)\,\widetilde{z} + \Xi\Delta/(4\,\widetilde{z})$, which, when inserted into Eq. (4), leads to the ideal gas profile proposed in [26, 41]. Such an approach is expected to fail as soon as the afore discussed scale separation is violated, that is whenever $\Delta \neq 0$ [42]. This is confirmed in Fig. 3. On the other hand, the rather rough ch_0 picture significantly improves the agreement with Monte Carlo data, while the extended ch_6 description fares remarkably well (see Fig. 3). Extensive simulations have also been performed for larger Ξ values, confirming the accuracy of the ch_6 route for all values of the dielectric jump Δ, while the simple ch_0 description is also shown to be quite accurate. In view of the underlying physical hypothesis (such as the two dimensional assumption for the fluid of counter-ions), better justified for strongly coupled systems, the very good agreement at $\Xi = 10$ rather comes as a surprise. A similar remark holds for ch_0, a crude, but nonetheless trustworthy approximation. It is interesting to compare and contrast our theory with the approach of Reference [10] which also also relies on the idea of singling out a test particle. However, at variance with our treatment, a) the remaining ions are treated at the Poisson-Boltzmann level ; b) the approach is restricted to $\Delta = 0$, and thus to a regime where many-body effects are less pronounced; c) the numerical resolution of a highly non-linear partial differential equation is required, with subsequent numerical integration of some auxiliary potential. In contrast, our treatment is fully analytical, and reduces to three simple equations presented above.

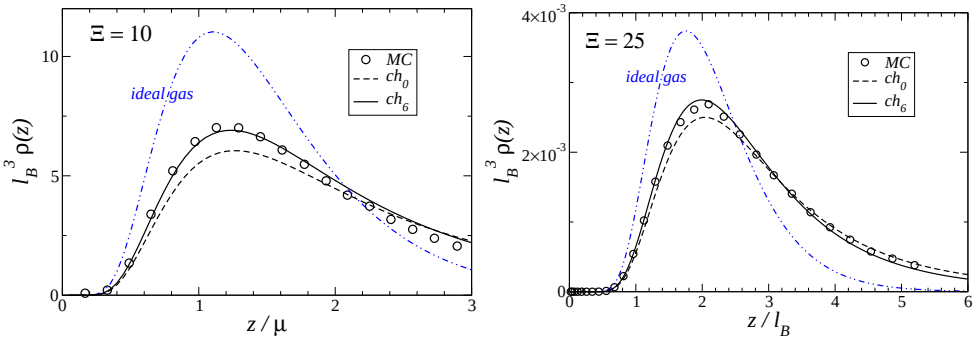

FIG. 3. Density profile of counter-ions for $\Delta = 0.95$ (meaning $\varepsilon/\varepsilon' \simeq 40$), $\Xi = 10$ (upper graph) and for $\Delta = 1$, $\Xi = 25$ (lower graph). The ch_0 and ch_6 predictions are compared to the ideal gas profile proposed in [26], and to the results of Monte Carlo simulations (taken from [26] for the upper graph). Here, $l_B = \beta e^2/\epsilon$ is the Bjerrum length.

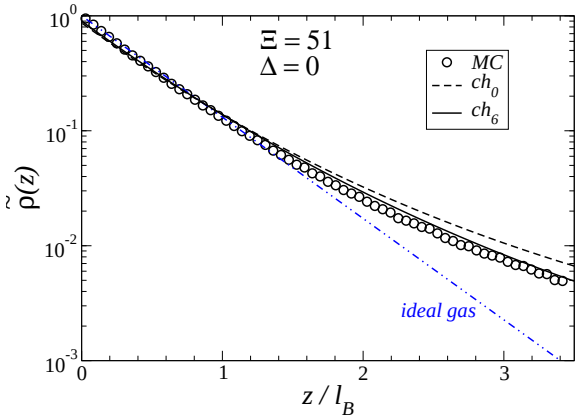

FIG. 4. Same as Fig. 3, without dielectric mismatch ($\Delta = 0$), and $\Xi = 51$. The density profile is maximum for $z = 0$, at contact with the plate: there is no depletion zone ($z^* = 0$).

It is of particular interest to analyze the well documented $\Delta = 0$ situation, where $\varepsilon = \varepsilon'$. There, the ideal gas view provides the dominant large coupling profile [11, 19, 21]. As seen in Fig. 4, both ch_0 and ch_6 perform significantly

better, and account correctly for the deviations from the exponential behavior: the overpopulated tail with respect to exponential behavior is a fingerprint of the repulsive effect of the fellow counter-ions forming a layer at $z \simeq 0$, that becomes more pronounced as the test particle moves away from this plane. We have found a similar agreement at $\Delta = 0$ for larger Ξ values.

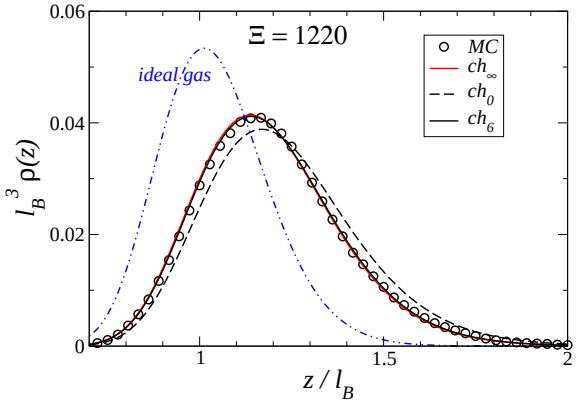

FIG. 5. Counter-ion profile at large coupling for $\Delta = 1$, symbols are the results of MC simulations. The "Wigner strong coupling" prediction (ch_∞) is also shown: it is almost indistinguishable from the ch_6 treatment.

Finally, we have tested our approach at very large couplings ($\Xi > 10^3$), see Fig 5. While the ideal gas picture of Refs. [26, 41] is inoperative, the ch_6 theory agrees well with the simulation data, in spite of the fact that the fluid of counter-ions is strongly modulated. We thus have considered extensions of ch_6, of the ch_n type, including a growing number of neighbors in the approach ($n = 6, 12, 18, 30 \ldots$), that we locate at their ground state position, in order to reach gradually the $\Xi \to \infty$ hexagonal arrangement. Pushing this logic, we show in Fig. 5 the ch_∞ prediction, where all ions are in their ground state position, except the test particle. It is still possible to compute analytically the resulting one body potential u making use of the lattice summation techniques developed in Ref. [43]. There is barely any difference between the ch_6 and the ch_∞ predictions. Incidentally, all ch_n formulations, for n between 6 and ∞, remain extremely close for all couplings we have investigated, which emphasizes the robustness of the approach [47]. Furthermore, the depletion zone extension, z^*, hardly depends on the level n in a ch_n treatment, from $n = 0$ up to $n \to \infty$!

V. CONCLUSION

In conclusion, we have presented a theory that accounts very accurately for the ionic density profiles of salt-free systems at moderate and strong couplings. Extensive comparisons with Monte Carlo simulations have been carried out. Our approach is accurate for $\Xi > 10$, and thus covers a wealth of experimentally relevant situations; for instance, DNA with trivalent counter-ions ($q = 3$) has Ξ around 100. The couplings that both evade mean-field and our analysis, namely Ξ in the range $[1, 10]$, must be addressed by computer simulation. Our formulation relies on basic electrostatics considerations, at variance with other more complex treatments such as the splitting field-theory [30, 34, 35, 48], and invokes transparent physical hypothesis pertaining to ionic correlations. The latter are accounted for at a one body level, which qualifies the approach as mean-field. Furthermore, besides accuracy, our treatment has been shown to be very robust. More complex geometries such as a slit, explored for small separations in Ref. [41] provide possible applications for the theory presented in this paper.

Another important perspective includes addition of co-ion [49], which brings an extra coupling parameter and hard core effects. This leads to significant complications, but can elaborate on the no-salt treatment presented here, in the spirit of previous approaches [50, 52]. On general grounds, salt ions "dress" the interactions between multivalent counterions [50], in a way that may be complex, but that may admit rather simple limiting laws. For instance, with highly asymmetric electrolytes, counter-ions may be in a strong coupling regime while coions are not. This leads to a picture where the counterions interact through a screened potential, which allows further progress [50]. Alternatively, if coions themselves are stronly coupled, they will form Bjerrum pairs with the counter-ions, leading to a system with excess counter-ions and a number of dipoles, see e.g. [51]. In a first approximation, neglecting from pairs [52], the formalism presented here is directly applicable.

The support received from the Grant VEGA No. 2/0015/15 and from CNPq, INCT-FCx, and US-AFOSR under the grant FA9550-16-1-0280 is acknowledged.

[1] G. L. Gouy, J. Phys. **9**, 457 (1910).
[2] D. L. Chapman, Philos. Mag. **25**, 475 (1913).
[3] P. Debye and E. Hückel, Phys. Zeitschr. **24**, 185 (1923).
[4] P. Linse and V. Lobaskin, Phys. Rev. Lett. **83**, 4208 (1999).
[5] J. Z. Wu, D. Bratko, H.W. Blanch, and J. M. Prausnitz, J. Chem. Phys. **111**, 7084 (1999).
[6] W. M. Gelbart, R. F. Bruinsma, P. A. Pincus and V. A. Parsegian, Phys. Today **53**, 38 (2000).
[7] F. J. Solis and M. O. de la Cruz, Phys. Today **54**, 71 (2001).
[8] A. Y. Grosberg, T. T. Nguyen and B. I. Shklovskii, Rev. Mod. Phys. **74**, 329 (2002).
[9] Y. Levin, Rep. Prog. Phys. **65**, 1577 (2002).
[10] Y. Burak, D. Andelman and H. Orland, Phys. Rev E **70**, 016102 (2004).
[11] A. Naji, S. Jungblut, A. G. Moreira, and R. R. Netz, Physica A **352**, 131 (2005).
[12] R. Messina, J. Phys.: Condens. Matter **21** 113102 (2009).
[13] D. Henderson and L. Blum, J. Chem. Phys. **69**, 5441 (1978).
[14] D. Andelman, in *Soft Condensed Matter Physics in Molecular and Cell Biology*, edited by W. C. K. Poon and D. Andelman (Taylor & Francis, New York, 2006).
[15] T. Palberg, M Medebach, N Garbow, M Evers, A Barreira Fontecha, H Reiber and E Bartsch, J. Phys.: Condens. Matt. **16**, S4039 (2004).
[16] When $\Delta > 0$, $\mu' \neq \mu$; it can be shown that $\mu' \propto \mu\,\Xi^{1/4}$ at large Ξ [24].
[17] I. Rouzina and V. A. Bloomfield, J. Phys. Chem. **100**, 9977 (1996).
[18] B. I. Shklovskii, Phys. Rev. E **60**, 5802 (1999); Phys. Rev. Lett. **82**, 3268 (1999).
[19] A. G. Moreira and R. R Netz, Phys. Rev. Lett. **87**, 078301 (2001); Eur. Phys. J. E **8**, 33 (2002); R. R. Netz, Eur. Phys. J. E **5**, 557 (2001).
[20] E. Trizac and L. Šamaj, arXiv:1210.5843, Lecture notes of the International School on Physics 'Enrico Fermi': Physics of Complex Colloids, Varenna, Italy, July 3-13 2012, Proceedings of Course CLXXXIV.
[21] L. Šamaj and E. Trizac, Phys. Rev. E **84**, 041401 (2011).
[22] M. Baus and J.-P. Hansen, Phys. Rep. **59**, 1 (1980).
[23] J. D. Jackson, *Classical Electrodynamics*, 3rd ed. (Wiley, New York, 1999).
[24] L. Šamaj and E. Trizac, Contrib. Plasma Phys. **52**, 53 (2012).
[25] L. Onsager and N. Samaras, J. Chem. Phys. **2**, 528 (1933).
[26] A. G. Moreira and R. R. Netz, Europhys. Lett. **57**, 911 (2002).
[27] S. Nordholm, Chem. Phys. Lett. **105**, 302 (1984).
[28] M. C. Barbosa, M. Deserno and C. Holm, Europhys. Lett. **52**, 80 (2000).
[29] A. V. Dobrynin and M. Rubinstein, J. Phys. Chem. B **107**, 82601 (2003).
[30] M. M. Hatlo and L. Lue, EPL **89**, 25002 (2010).
[31] This leaves a Ξ-gap between 1 and 10 where no analytical theory has been proposed, while $\Xi < 1$ is covered by the Poisson-Boltzmann theory.
[32] J.-P. Hansen and I. R. McDonald, *Theory of Simple Liquids*, Academic Press, 2006.
[33] In $g(\mathbf{r})$, the vector $\mathbf{r}$ is two-dimensional, measuring ion separation parallel to the interface.
[34] Y. G. Chen and J. D. Weeks, Proc. Natl. Acad. Sci. U.S.A. **103**, 7560 (2006); J.M. Rodgers, C. Kaur, Y.G. Chen and J.D. Weeks, Phys. Rev. Lett. **97**, 097801 (2006).
[35] C. D. Santangelo, Phys. Rev. E **73**, 041512 (2006).
[36] A. Bakhshandeh, A. P. dos Santos, and Y. Levin, Phys. Rev. Lett. **107**, 107801 (2011).
[37] Each ion is surrounded by a first shell of nearest neighbors which defines the coordination number in the liquid. Interestingly, this coordination number is very close in the liquid and crystalline phases [53].
[38] In Ref. [36], both steps were merged, resulting in a double-layer where all counter-ions move coherently, which is unphysical. It is important to disentangle the calculation of the optimal distance z^* from that of the effective one-body potential u.
[39] In line with the argument given in the caption of Fig. 1, $\sigma a^2 \propto q$. The prefactor $3^{-1/4}\sqrt{2}$ is chosen so that a coincides with the lattice constant in the crystalline phase, a triangular (hexagonal) arrangement. The a thus defined also provides an excellent measure of the nearest neighbor typical distance in the liquid phase [19].
[40] We sum the interactions between the test particle and its 6 nearest neighbors at a distance $\sqrt{(z-z^*)^2+a^2}$, their images at a distance $\sqrt{(z+z^*)^2+a^2}$, the particle self-image at a distance $2z^*$, and the two punctured plates at $\pm z^*$, having hole radius R_6.
[41] Y. S. Jho, M. Kanduc, A. Naji, R. Podgornik, M. W. Kim and P. A. Pincus, Phys. Rev. Lett. **101**, 188101 (2008).
[42] A more precize criterion for the validity of the ideal gas picture is $z^* \ll a$. This can be met for small enough Δ at large coupling, but is incorrect for Δ above 0.3.
[43] L. Šamaj and E. Trizac, Phys. Rev. B **85**, 205131 (2012).
[44] A. P. dos Santos and Y. Levin, *Electrostatics of Soft and Disordered Matter*, Ch. 14 (CRC Press, Boca Raton, 2014).

[45] A. P. dos Santos and Y. Levin, J. Chem. Phys. **142**, 194104 (2015).
[46] A. P. dos Santos, M. Girotto, and Y. Levin, J. Chem. Phys. **144**, 144103 (2016).
[47] This is a distinctive feature compared to previous approaches such as Ref. [36], where increasing the number of discrete neighbors results in poor predictions.
[48] L. Lue and P. Linse, J. Chem. Phys. **142**, 144902 (2015).
[49] M. Kanduč, M. Trulsson, A. Naji, Y. Burak, J. Forsman, and R. Podgornik, Phys. Rev. E **78**, 061105 (2008); M. Kanduč, A. Naji, J. Forsman, and R. Podgornik, J. Chem. Phys. **132**, 124701 (2010).
[50] M. Kanduč, A. Naji, J. Forsman, and R. Podgornik, Phys. Rev. E **84**, 011502 (2011).
[51] A. P. dos Santos, A. Diehl and Y. Levin, J. Chem. Phys. **132**, 104105 (2010).
[52] F. Paillusson and E. Trizac, Phys. Rev. E **84**, 011407 (2011).
[53] P. F. Damasceno, M. Engel and S. C. Glotzer, Science **337**, 453 (2012).